

Tryptophan Fluorescence of Mitochondrial Uncoupling Protein

P JEZEK¹, P LILLO² AND J POLFCHA¹

¹ *Department of Membrane Transport Biophysics,
Institute of Physiology Academy of Sciences of the Czech Republic
Videňská 1083 14220 Prague 4 Czech Republic*

² *Instituto de Química Física Rocasolano C S I C
Calle Serrano 119 28006 Madrid, Spain*

Abstract. Mitochondrial uncoupling protein (UcP) contains two tryptophans buried in transmembrane α -helices Trp-173 at the matrix end of fourth α -helix and Trp-280 on the sixth α -helix. However, the steady-state emission of isolated UcP exhibited properties unusual for α -helices: maximum close to that of free tryptophan emission and low quantum yield of 0.04. The former suggests prevailing tryptophan contacts with hydrophilic residues and confirms Trp-173 proximity to the water/membrane interface and Trp-280 location near a water-filled nucleotide-binding-site cavity. The latter might indicate that transmembrane segments are not true α -helices. Measured depolarization factor of 0.6 suggests also their 'breathing'.

Analysis of UcP emission decays measured by time-correlated-single-photon-counting, yielded components 0.4–0.6 ns, 2.2–3 ns and 9–10 ns (or alternatively 0.1–1.5, 4.3 and 12.2 ns or 0.1–0.3, 1.2–3.7 and 10.5 ns), very similar to those of free tryptophan in water, where the longest component belongs to anionic form. Hence, such an 'anionic' conformation must exist in UcP, perhaps as a consequence of charge-transfer complexes between Trp-173 & Lys-174 and Trp-280 & Arg-276. Moreover, N-ethylmaleimide modification, known to induce conformational changes, prolonged the 10 ns component, decreased quantum yield to 0.03 without changes in emission spectra, while slightly shifting absorption to red and increasing tyrosine exposure to water.

Key words: Intramembrane tryptophans – Integral membrane proteins – Mitochondrial uncoupling protein – Time-correlated-single-photon-counting

Correspondence to Dr Petr Ježek, Dept. No. 375, Membrane Transport Biophysics, Institute of Physiology, Academy of Sciences of the Czech Republic, Videňská 1083, 14220 Prague 4, Czech Republic. Fax: (+420 2) 4752488, E-mail: jezek@sun1.biomed.cas.cz

Abbreviations: MOPS 4-morpholinopropanesulfonic acid NEM N-ethylmaleimide OctylPOE octylpentaoxyethylene UCP uncoupling protein

Introduction

Tryptophan fluorescence in proteins provides an intrinsic probe useful to understand some structure/function relationships. Nevertheless, the time resolved emission of protein tryptophans is complex (e.g. Beechem and Brand 1985, Efting et al 1987, Szymanski et al 1988, Peng et al 1990, Chabbert et al 1991, Kawata and Hamaguchi 1991, Varley et al 1991, Lakowicz and Gryczynski 1992, Kim et al 1993, Hasselbacher et al 1995, Ladokhin and Holloway 1995) and has not been fully understood. This is also valid for tryptophans in membrane proteins (e.g. Ferreira and Verjovski-Almeida 1989, Klemfeld 1989, Bigelow and Inesi 1991, Ladokhin et al 1991, Lakey et al 1991, Gonzalez-Manas et al 1993, Rodionova et al 1995). It has been shown that a complex decay pattern observed even with a single Trp residue in a protein exists because of the excited state heterogeneity (Kim et al 1993). This might reflect a multi-set pattern of general energy transfer on subpopulations of the conformational states of the given protein. It is argued on what is the primary cause of the complex Trp emission decay. Is it a ground state heterogeneity given by *a priori* existence of the conformational states? Or is it *a priori* existing ever changing pattern of multimodal energy transfer of all kind (not only Forster type) which proceeds during the lifetime of the excited Trp state? Some well documented cases support rather the latter point of view (Kim et al 1993). Consequently, in the case of two-Trp-containing proteins, it is almost impossible to ascribe discrete decay components to the particular residues, unless additional effects cause a "very specific" emission of one of them. The situation in a dynamic protein is somewhat analogous to that of free tryptophan in aqueous solution at pH 7. Trp exists in a form of two different rotamers and the anionic form producing a corresponding triple-exponential emission decay (Creed 1984a). Besides the major influence of the conformational dynamics, some other specific effects may contribute to the nature of Trp emission. For example, the hydrophobic environment leads to a blue-shifted Trp emission, usually for Trp located deeply in the protein core. Moreover, Trp located in the regular α -helices usually exhibits high quantum yields (Beechem and Brand 1985, Chabbert et al 1991).

The uncoupling protein (UCP) of brown adipose tissue mitochondria is a model prototype of an integral membrane protein, suitable for studies of structure/function relationships (Klingenberg 1990, Nedergaard and Cannon 1992, Jeřek et al 1998). UCP belongs to the gene family of dimeric mitochondrial anion porters with homologous triad sequences that determine six transmembrane α -helices *per* monomer (Klingenberg 1990). Having most of their structure embedded in the membrane, short cytosolic and much longer matrix segments, these carriers repre-

sent typical integral membrane proteins. The α -helical structure in a 50% proportion has been documented in UCP by Rial et al. (1990). UCP translocates anions in a uniport mode (Jeřek and Garlid 1990). It forms a purine nucleotide-sensitive pathway with a strict specificity to monovalent unipolar anions (Jeřek and Garlid 1990) including fatty acids. Physiologically, UCP probably mediates fatty acid cycling leading to H^+ uniport and consequently, to the uncoupling of mitochondria (Garlid et al. 1996; Jeřek et al. 1997a,b, 1998). UCP contains two tryptophans, Trp-173 and Trp-280. Trp-173 is located at the matrix end of the fourth *trans*membrane α -helix. Trp-280 lies in the middle of its sixth *trans*membrane α -helix that aligns the nucleotide binding domain (Klingenberg 1990; Mavinger and Klingenberg 1992; Modriansky et al. 1997). The UCP intrinsic fluorescence has been studied by Viguiera et al. (1992) but as shown in this study, their data had to be re-evaluated.

In this work, we analyzed basic absorption and steady-state emission properties of UCP intrinsic fluorescence which was also studied by the time-correlated-single-photon counting. We demonstrate that, although located on α -helices, UCP tryptophans possess properties surprisingly similar to that of the free tryptophan.

Materials and Methods

Chemicals were purchased mostly from Sigma (St. Louis, USA). Hydroxylapatite BIO-GEL HTP was from Bio-Rad (Richmond, USA). Octylpentaooxyethylene was from Bachem Feinchemikalien (Bubendorf, Switzerland). Brown adipose tissue was excised from Syrian hamsters cold-adapted for three weeks at 5°C.

Isolation of the uncoupling protein

Isolation of UCP on hydroxylapatite was done without the lipid protection from brown adipose tissue mitochondria (control or NEM-pi-modified) extracted with 4.5% detergent octylpentaooxyethylene (OctylPOE), in 20 mmol/l Na-MOPS, 50 mmol/l Na_2SO_4 , 0.2 mmol/l Na-EDTA, pH 6.7, followed by stepwise elution (Jeřek and Freisleben 1994). Purity, determined by staining, reached over 90% as detected by SDS-PAGE on silver-stained gels ('Mighty Small II', Hoefer Sci., San Francisco, USA). UCP was reconstitutively active in this form (Jeřek and Freisleben 1994; Garlid et al. 1996; Jeřek et al. 1997b). Moreover, UCP intactness in the detergent (retained GDP binding capacity) usually lasts for 1 or 2 days at room temperature (Lin and Klingenberg 1982) which allows quite long measurements.

Absorption spectra

Absorption of UCP in a detergent-micellar solution was measured first on a Cary 219 (Varian, Walton-on-Thames, UK) double-beam spectrophotometer for evaluation of quantum yields. Samples in 0.5 × 0.5 cm fluorescence quartz cuvettes were

tested for absorbance immediately after running the fluorescence spectra. The elution buffer with 2% OctylPOE was used as a blank. The slits were set to 1 or 2 nm for scanning speed of 0.2 or 0.5 nm/s, respectively. Equal slits were used for the emission spectra (see below). The second instrument was a diode-array uv-spectrophotometer Spectronic 3000 (Milton Roy, Rochester, USA). A baseline (cf. above) was taken immediately before the measurement. The scan-time period was 8.2 s. Second derivative spectra were obtained using the software package provided by Milton Roy.

Absorbance values from both instruments were affected by the light scattering on the sample, pronounced as non-zero absorbance in the region above 400 nm where Trp should have zero absorbance. At 295 nm, light scattering represented more than two thirds of the apparent signal. Hence, the light scattering contribution was simulated theoretically (Shih and Fasman 1972) as follows:

$$OD = 10^N \lambda^M \quad (1)$$

where the constants N and M were determined from the best fits of the theoretical curves to the experimental traces in the region 400–500 nm (for Spectronics) and 360–400 nm (for Cary). A fitting procedure using a Marquadt algorithm was employed.

Second derivative absorption for determination of tyrosine exposure

Absorbance around 270 nm is due to Trp and Tyr absorption, while in proteins usually the former exceeds the latter (Beechem and Brand 1985). The state of Tyr residues can be evaluated by the second derivative absorption spectroscopy (Ragone et al. 1984), estimating the heights between the second-derivative positive and negative peaks—the arithmetic sums at 285 vs. 288 nm (**a**) and 291 vs. 295 nm (**b**). The ratio **a/b** is then a factor that reports the exposure of Tyr residues to the water environment. In model peptides and in some proteins, the ratio reaches a constant value of about 2/3 (Ragone et al. 1984). Higher Tyr exposures or protein denaturation increase this ratio.

Steady state fluorescence

Tryptophan fluorescence can be exclusively excited at 295 nm or higher wavelengths, since tyrosine has virtually no absorbance at 295 nm (Beechem and Brand 1985; Creed 1984a). Steady-state fluorescence was measured by a photon-counting mode on an SLM 8000D (SLM Inc., Urbana, USA) with a double grating excitation monochromator. Polarizers of Glan-Thompson-type were set in vertical position (excitation) and in the 'magic angle' (54.7°) (emission). Both excitation slits were set at 2 nm, and emission slits at 1 or 2 nm. At the employed integration constant of 10 s, the dark counts were 25 per s. Collected spectra (step 1 nm) were

corrected for the instrument response using the evaluated correction function for isotropic fluorescence (Acuna and Lillo unpublished). This procedure was justified since it yielded results equal to the total fluorescence calculated from the polarized emission ($I_{\perp} = I_{\parallel} + 2I_{\perp}$) and the corresponding corrections for I_{\parallel} and I_{\perp} .

Quantum yield (Q) of UCP tryptophans was determined relative to the solution of 50 $\mu\text{mol/l}$ Trp in 10 mmol/l Tris-HCl pH 6.9, for which a value of 0.14 was taken (Bishai et al. 1967, Werner and Forster 1978). Necessary integrals of the corrected photon-counting emission spectra were calculated, so that Q was calculated as follows:

$$Q_{(\text{UCP-Trp})} = \frac{0.14 \cdot A_{(295\text{nm})}^{\text{Trp}} \int (\text{Emission UCP}) d\lambda}{A_{(295\text{nm})}^{\text{Trp}} \int (\text{Emission Trp}) d\lambda} \quad (2)$$

As discussed above, UCP absorbance at 295 nm ($A_{(295\text{nm})}^{\text{Trp}}$) was the parameter most sensitive to systemic error.

Time resolved fluorescence

Time resolved fluorescence intensity decays were measured on an Ortec 9200 Nanosecond fluorescence spectrometer (EG&G Princeton USA). A thyatron gated nitrogen ns-flash lamp (Edinburgh Instruments, Edinburgh UK) with a repetition frequency of 50 kHz, operating at 5.5 kV, was used as a light source. The N_2 bands 294 and 297 nm were selected by a single-grating monochromator (Jobin Yvon Longjumeau France) set at 295 nm slit 16 nm. The excitation polarizer was oriented vertically while the emission polarizer was set at 54.7°. Trp emission was selected using the cut-off filters 318 nm or in specific cases 345 nm (Schott Glaswerke Mainz Germany). A blue-portion of emission was selected by using a UG5 Schott filter which transmits light between 200 and 400 nm simultaneously with a 318 nm cut-off filter. It was compared to the results when using only a U360 Schott filter transmitting between 300–400 nm.

Emission was detected with a Phillips XP2020Q photomultiplier (Groningen Netherlands), and the decay was resolved by a time-amplitude converter and an Ortec Model 6240B Multichannel analyzer with 0.105 ns per channel (255 channels) interfaced to a personal computer. The decay function was counted to a minimum of 10,000 ideally 20,000 counts in the peak channel. The background signal was recorded separately with a sample of an elution buffer containing 2% OctylPOE. The instrument response function was recorded as a flash lamp pulse passed through a Ludox scatterer solution under the same conditions but without the cut-off or color filters. Using a software developed by P. Lillo, data were fitted with model functions generated by convolution of the instrument response function and an n -component exponential decay functions. The software involved correction for the stop photomultiplier 'color shift'. The discrete n -exponential decay model was

accounted for as follows

$$I(t) = \sum_i (\alpha_i \exp(-t/\tau_i)) \quad \text{with} \quad \sum_i \alpha_i = 1 \quad (3)$$

The lifetime components τ_i and amplitudes α_i were obtained from best fits, judged by reduced χ^2 weighted residuals, and an autocorrelation function of the residuals. The mean fluorescence lifetime $\langle\tau\rangle$ was taken as the first order mean

$$\langle\tau\rangle = \sum_i (\alpha_i \tau_i) \quad (4)$$

and fraction contribution to the total intensity is given by

$$f_i = \alpha_i \tau_i / \sum_i (\alpha_i \tau_i) \quad (5)$$

Steady-state anisotropy measurement

The Azumi and McGlynn (1962) procedure was used to obtain steady-state anisotropy

$$r = (I_{VV} - I_{VH} - U) / (I_{VV} + 2I_{VH} - U) \quad (6)$$

where $U = I_{HH} / I_{HH}$, and indexes V and H describe the vertical and the horizontal orientation of polarizers, when the position of excitation polarizer is indicated by the first index (V , vertical, H horizontal), and the emission polarizer by the second index

Results

Absorption of native and N-ethylmaleimide-modified uncoupling protein

Absorption spectra of native UCP¹ (control) and UCP chemically modified with N-ethylmaleimide (NEM) in a OctylPOE micellar solution were evaluated, thanks to the zero absorbance of the detergent above 220 nm. Absorption maxima were around 270 nm (Fig. 1) and at 214–218 nm (not shown). The first absorption maximum of experimental spectra for native UCP appeared either as a shoulder at 265 nm or as a distinct peak at 265–267 nm, depending on the extent of light scattering. With NEM-modified UCP, the absorption maximum was slightly red-shifted and the distinct peak at 268–270 nm was resolved (Fig. 1). NEM binds to residues at the entry of the GDP-binding site cavity and is supposed to induce a major conformational change (Winkler and Klingenberg 1992), while it prevents

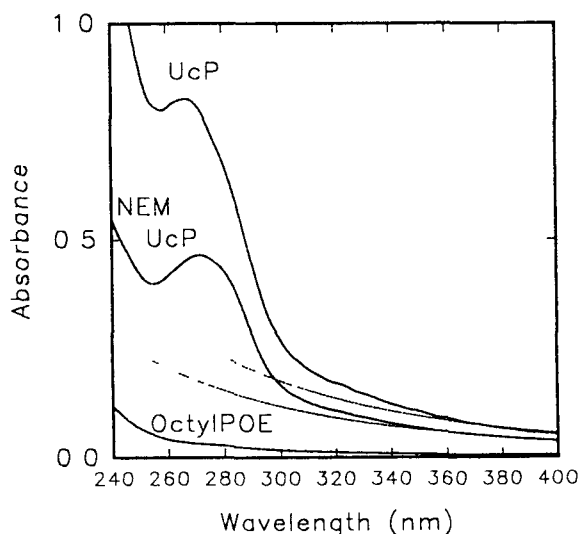


Figure 1. Absorption spectra of control and NEM labeled uncoupling protein. Spectra of uncoupling protein in a micellar solution of detergent OctylPOE were measured on a diode-array spectrophotometer (0.33 nm resolution) at 0.047 mg/ml (control) and 0.023 mg/ml (NEM-labeled UcP) with regard to a reference containing 2% OctylPOE. The bottom trace shows the absorption spectrum of 2% OctylPOE taken vs. distilled water background. The dotted lines represent calculated contribution of light scattering (cf. Methods).

GDP binding and gating. This conformational change is reflected by the observed absorption red shift.

The dotted lines in Fig. 1 illustrate the contribution of light scattering calculated according to Eq. 1. The protein was a source of additional scattering above the level obtained with the sole detergent. On the contrary, scattering on a detergent solution multiplied by a determined coefficient matched the theoretical calculations. GDP as a UcP inhibitor and ligand did not influence either the position of the absorption maximum or the protein absorbance (not shown) as revealed using references containing the same amount of GDP (30 or 300 $\mu\text{mol/l}$, respectively).

Second derivative absorption of native and N-ethylmaleimide modified UcP

UcP contains 9 Tyr and 2 Trp; therefore, a minor portion of absorbance at 270 nm may be due to tyrosines. The state of Tyr residues was evaluated by the second derivative absorption spectroscopy. In the case of UcP the ratio a/b (cf. Methods) was found to fall into a range between 1.0–2.2 (15 evaluations with 3 UcP preparations) and with NEM modification it slightly increased to 1.3–2.5 (Fig. 2). An a/b

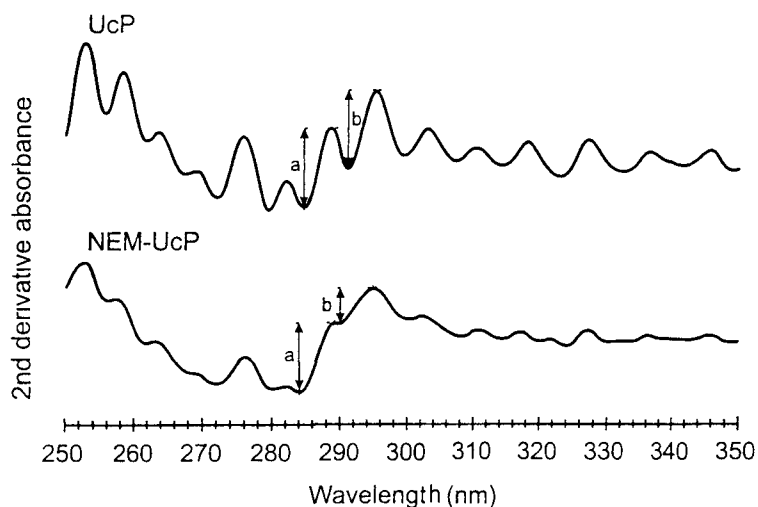


Figure 2. Second derivative spectra of uncoupling protein. Second derivative of absorption spectra are plotted for control and NEM-labeled UcP. The parameters *a* and *b* (cf Methods) are indicated by arrows. In the samples shown, the ratio *a/b* reached the magnitude of 1.05 and 1.87 in native and NEM-labeled UcP, respectively.

ratio higher than 2/3 indicates aqueous surroundings of UcP tyrosines. For UcP, it reflects the location of Tyr1 residues in the matrix water-exposed segments. In NEM-UcP, the mild increase in this ratio shows that the corresponding conformational change is not extensive (denaturation-like).

Steady state fluorescence of the uncoupling protein

By using steady-state photoncounting and omitting polarizers, the data reported previously (Viguiera et al. 1992) could be confirmed, with the maximum of the corrected emission spectrum of UcP tryptophans at 332 nm (not shown). However, when vertically polarized light was used for excitation and the emission polarizer was set at the magic angle (54.7°) to count the true total intensity, the maximum of the corrected spectrum was found at 343 nm in control (Fig. 3) and at 345 nm in NEM-UcP (not shown). The difference with regard to the measurement without polarizers can be due to the existence of Trp conformers having different lifetimes and spectral maxima. Without counting the total fluorescence intensity, anisotropy might enhance the contribution of the lower wavelength component. It might be concluded that Trp emission in UcP is only slightly blue-shifted when compared with that of free tryptophan at neutral pH, which has a maximum at 349 nm (Fig. 3) (Creed 1984a, Lakowicz 1984, Beechem and Brand 1985). However,

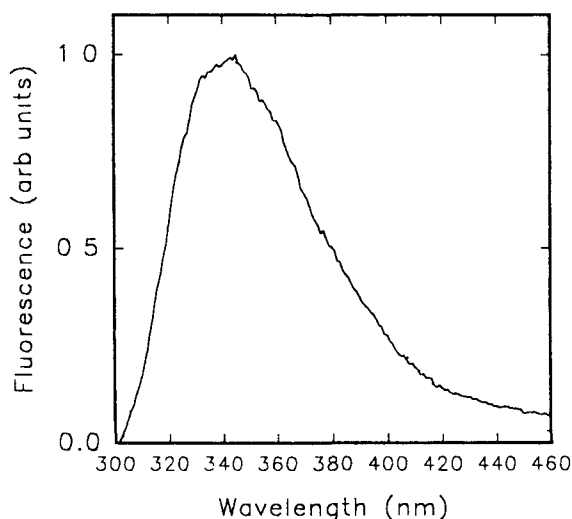


Figure 3. Emission spectrum of the isolated uncoupling protein as compared with the spectrum of free tryptophan. Corrected emission spectra measured by steady-state photoncounting with polarizers oriented at a "magic angle", 54.7° are shown for isolated UcP (solid line, 0–125 mg protein/ml) and 50 $\mu\text{mol/l}$ tryptophan in 10 mmol/l Tris-HCl, pH 6.9 (dotted line). Maximum of UcP emission appears at 343 nm for Trp emission at 349 nm. All slits were adjusted to 2 nm and the integration time of photoncounting was set to 10 s. The background given by light scattering on 2% OctylPOE solution was subtracted from the measured spectrum and the difference was corrected for the spectral response of the instrument (cf. Methods).

temperature-denaturated UcP in OctylPOE exhibited a red shift to 350 nm (not shown). Therefore, the intactness of the samples can be judged upon from their emission maxima, and this has been routinely used.

The quantum yield determined from two absorption and four corrected emission spectra was calculated as 0.045 ± 0.004 for the first UcP sample and 0.041 ± 0.001 for the second UcP sample. Quantum yield did not significantly change upon GDP binding. However, NEM-modified UcP exhibited a lower quantum yield of 0.031 ± 0.003 . This indicates the presence of additional modes of energy transfer or non-radioactive decay processes, and again illustrates conformational changes resulting from NEM-modification.

Tyrosine fluorescence was studied using excitation at 275 nm, while the net Trp spectra (excitation at 295 nm) were subtracted from it. The resulted net tyrosine spectra had maximum intensities reaching 30–50% of the total emission intensity at 275 nm excitation, and exhibited red-shifted maxima around 310 nm (not shown). The usual Tyr emission maximum lies at 305 nm (Creed 1984b).

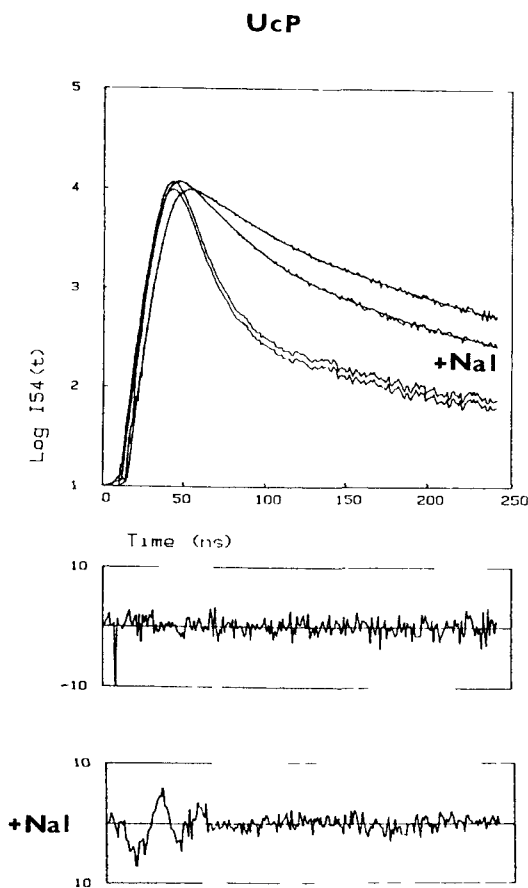


Figure 4. Decay kinetics of tryptophan emission of the isolated uncoupling protein. Top traces: control; lower traces: 0.8 mol/l NaI added. Top panel shows the instrument responses, emission decays with the subtracted background, and then best fits using the model of three-exponentials (solid lines); the middle and the bottom panels show residuals of the two respective fits.

The excitation wavelength was set at 295 nm (slit 16 nm) with vertical polarization; emission was collected through a 318 nm cut off filter and a polarizer oriented at 54.7° . The fit of the control emission decay gave the following parameters: α_1 0.453, τ_1 0.65 ± 0.01 ns, α_2 0.421, τ_2 2.96 ± 0.23 ns, α_3 0.126, τ_3 8.6 ± 0.6 ns ($\chi^2 = 1.37$). The contributions to the steady-state fluorescence were 11.5%, 47.3% and 41.2% respectively. The fit of the unquenched emission decay in the presence of 0.8 mol/l NaI yielded the following parameters: α_1 0.941, τ_1 0.60 ± 0.02 ns, α_2 0.051, τ_2 1.83 ± 0.05 ns, α_3 0.008, τ_3 6.5 ± 0.2 ns, with the steady-state contributions of 27.6%, 45.6% and 26.7% respectively, and with χ^2 of 1.33, when the background of light scattering on 2% OctylPOE was not subtracted. When the background of up to 30% of peak counts was subtracted, the resulted fit gave α_1 0.99, τ_1 0.01 ± 0.01 ns, α_2 0.001, τ_2 1.3 ± 2 ns, α_3 0.006, τ_3 2.3 ± 0.2 ns, with steady-state contributions of 30%, 2.8% and 67.4% respectively, and χ^2 of 5.

Table 1. Typical three-exponential fits of the UcP fluorescence intensity decay. Typical fits of tryptophan emission decay as selected from 8 measurements with control and 12 measurements with NEM-labeled UcP. Measurements were performed as described in legend to Fig. 4. When indicated, Schott filter UG 5 was used, or cut off filter (c/o) 345 nm instead of the filter that was used routinely, the cut off filter 318 nm.

SAMPLE	τ_1	τ_2	τ_3	α_1	α_2	α_3	χ^2
Control two exponential model	0.18	5.25					12.2
Control	0.66 \pm 0.07	2.90 \pm 0.23	8.60 \pm 0.64	0.453	0.421	0.126	1.37
c/o345	1.00 \pm 0.36	2.35 \pm 0.25	10.59 \pm 0.46	0.239	0.594	0.167	2.04
0.8 mol/l NaI backgrnd not subtr	0.18 \pm 0.01	1.84 \pm 0.05	6.46 \pm 0.17	0.834	0.142	0.024	1.20
0.8 mol/l NaI backgrnd subtracted	0.43 \pm 0.05	1.46 \pm 0.11	3.71 \pm 0.08	0.450	0.373	0.178	1.58
Control +GDP	0.07 \pm 0.01	2.21 \pm 0.05	8.08 \pm 0.16	0.892	0.083	0.024	1.58
NEM-UcP	0.39 \pm 0.03	2.49 \pm 0.08	9.71 \pm 0.24	0.498	0.369	0.133	1.27
UG-5	0.40 \pm 0.04	2.62 \pm 0.11	10.46 \pm 0.39	0.483	0.389	0.127	1.16
0.8 mol/l NaI backgrd not subtr	0.27 \pm 0.01	1.88 \pm 0.04	7.42 \pm 0.15	0.696	0.257	0.047	1.46
0.8 mol/l NaI backgrd subtracted	0.43 \pm 0.28	1.75 \pm 0.14	5.26 \pm 0.20	0.384	0.497	0.118	1.60

Time resolved fluorescence of the uncoupling protein

As shown in Fig. 4 and Table 1, the decay of Trp emission in UcP is multiexponential. Two-exponential models were unsatisfactory to fit the data (Table 1), and the best fits were obtained using at least a three-component exponential model (8 measurements with 3 UcP preparations). In these deconvolutions, the first component (τ_1) ranged between 0.3 and 0.6 ns (fits with $\tau_1 < 0.2$ ns were ignored because of the time resolution of the instrument). The second component (τ_2) was between 2.1–2.9 ns. The third component (τ_3) showed more variability among UcP samples and ranged from 8.6 ns up to 9.6 ns. When only the red-portion of Trp emission was collected using the 345 nm cut-off filter, it was possible to resolve the decay into components of 1, 2.4 and 10.6 ns. Probably states with a shorter lifetime and emission maxima below 340 nm were eliminated. The decay pattern did not differ

much in the presence of GDP (Table 1). With UCP modified by NEM (Fig. 5, Table 1, 12 measurements), the value of τ_1 was between 0.4–0.5 ns, τ_2 ranged between 2.2–2.8 ns, and τ_3 was between 9.7–11 ns. Note that τ_3 was slightly longer than in control UCP.

The proportions of the different components were similar in all fits for control and NEM-labeled UCP (Table 1). The shortest component had a minimum contribution to the steady-state emission. The mean lifetime (τ) was 1.8–2.6 ns and 2–2.9 ns for control and NEM-UCP, respectively. The slightly longer decay explains the lower quantum yield of NEM-modified UCP. To verify the lack of a systemic error, we also measured decays in the presence of the “UG5” color filter that cuts off the very-red tail of Trp emission and strongly eliminates the second harmonic of the light source. The obtained decay parameters were almost identical (Table 1). In addition, decays of UCP emission (not shown) which yielded identical components were obtained with two additional devices in Prague and using a demonstration unit of OB 900 Lifetime spectrometer of Edinburgh Instruments (UK).

UCP emission decay in the presence of 0.8 mol/l NaI was also characterized. Under these conditions a Trp population of about 2/3 is supposed to be quenched (Viguiera et al. 1992), hence in the case of dynamic quenching, a lifetime reduction by 66% would be expected. However, due to possible heterogeneity of the sample as reflected by the existence of 33% unquenchable emission, the expected reduction might be only up to 55%. Indeed, the decays in the presence of 0.8 mol/l NaI were extensively shortened in both control and NEM-modified UCP (Figs. 4–5, Table 1). When the background was not subtracted, deconvolutions (Figs. 4, 5) yielded τ_3 of about 5.4–6.5 ns in control and 7.4 ns in the NEM-modified UCP, while τ_2 was reduced to 1.8 ns and 1.8–2 ns, respectively. When the background signal (reaching up to 30% of the signal in quenched samples on the peak channel, χ^2 was about 1.6) was subtracted, the value of τ_3 was 2.3–2.4 and 3.7 ns and that of τ_2 1.3–0.7 and 1.6 ns, respectively (3 experiments, control), while τ_3 was 5.3 or 5.7 ns with the NEM-modified UCP. Thus, a lifetime reduction in the control sample reached its upper limit, whereas in NEM-modified UCP only a lower limit was attained.

The emission decays were also fitted using a model of four exponentials (τ_1^* to τ_4^* , Table 2). The value of τ_3^* was tentatively assigned to 3.7 or 5.3 ns, i.e. to match τ_3 values obtained in the presence of iodide (in control and NEM-UCP, respectively). The resulted deconvolutions with τ_4^* fixed at 10.5 ns gave better χ^2 than was the case of the three-exponentials model (Table 2). With only one component fixed (not shown) or without any defined constraint τ_3^* of 3–4 ns and τ_4^* of 10–12 ns were obtained with fits having χ^2 of 1.1 to 1.17. In conclusion, a complex combined emission of two UCP tryptophans (which might also reflect heterogeneity of their accessibility) can be resolved into four exponential components, and one of them is always a long component of about 10 ns. The proportional reduction of this component at 0.8 mol/l NaI indicates that this is not an artifact.

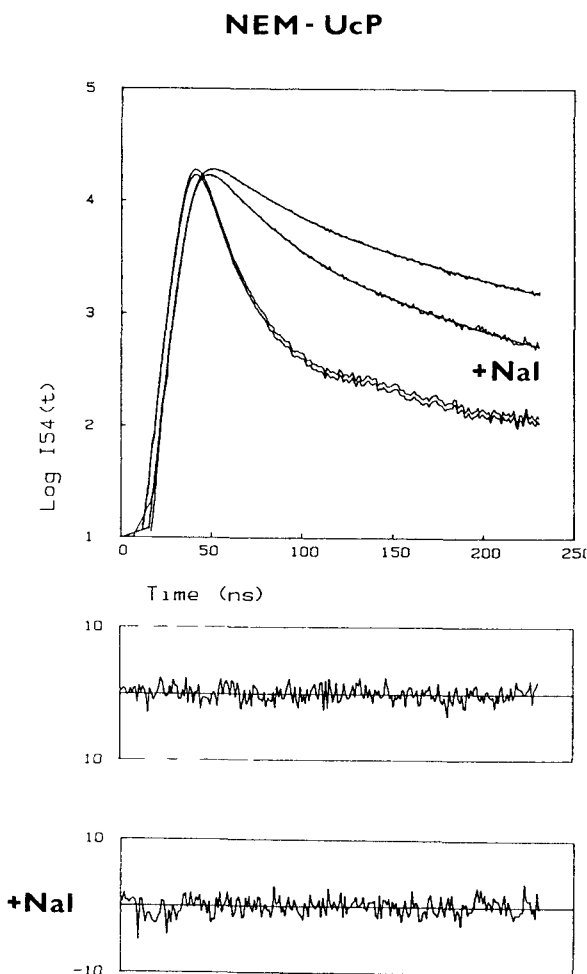


Figure 5. Emission decay kinetics of the isolated NEM-labeled uncoupling protein. Top traces: NEM-UCP; lower traces: 0.8 mol/l NaI added. Top panel shows the instrument responses (emission decays with subtracted background) and the best fits using the model of three-exponentials (solid lines); the middle and the bottom panels show residuals of the respective fits.

Conditions were identical as described in legend to Fig. 3. The fit of emission decay of Trp in NEM-labeled UCP gave the following parameters: α_1 0.498, τ_1 0.39 ± 0.03 ns, α_2 0.369, τ_2 2.49 ± 0.08 ns, α_3 0.133, τ_3 9.7 ± 0.2 ns ($\chi^2 = 1.26$); the contribution to the steady state fluorescence was 8%, 38.2% and 53.8% respectively. The fit of the decay of the unquenched portion in the presence of 0.8 mol/l NaI (background subtracted) yielded the following parameters: α_1 0.491, τ_1 0.47 ± 0.07 ns, α_2 0.407, τ_2 1.63 ± 0.07 ns, α_3 0.102, τ_3 5.8 ± 0.1 ns ($\chi^2 = 1.82$); the contributions to the steady state fluorescence were 15.4%, 44.7% and 39.9% respectively.

Table 2. The best four exponential fits of the UeP tryptophan fluorescence intensity decays. The parameters marked ^{fix} were introduced as constants assuming the fourth component constant of 10.5 ns and the third taken as a τ_3 yielded with 0.8 mol/l NaI. Normalized coefficients α_i are listed in parentheses and percentages to the steady-state contribution in square brackets.

SAMPLE	τ_1^*	τ_2^*	τ_3^*	τ_4^*	χ^2
Control					
First measurement	0.34 \pm 0.01 (0.266) [3.6%]	1.20 \pm 0.13 (0.314) [15%]	3.71 ^{fix} (0.348) [51%]	10.5 ^{fix} (0.072) [30%]	1.37
Second measurement	0.08 \pm 0.001 (0.633) [6.5%]	1.22 \pm 0.11 (0.175) [33%]	3.71 ^{fix} (0.157) [39%]	10.5 ^{fix} (0.034) [20%]	1.18
no constraint	0.12 (0.569) [4.7%]	1.46 \pm 0.4 (0.233) [23%]	4.3 \pm 1 (0.170) [49%]	12.2 (0.027) [23%]	1.17
NEM UeP	0.39 \pm 0.009 (0.482) [7.5%]	2.57 \pm 1.69 (0.385) [39%]	5.26 ^{fix} (0.009) [2%]	10.5 ^{fix} (0.124) [52%]	1.17
no constraint	0.02 \pm 0.05 (0.747) [1.7%]	0.79 \pm 0.18 (0.100) [10%]	3.14 \pm 0.34 (0.114) [42%]	12.0 \pm 1.4 (0.033) [46%]	1.10

Anisotropy of Trp emission in the uncoupling protein

Emission anisotropy of intrinsic fluorescence can refer to both the mobility of the protein and the segmental motion (Lakowicz 1984). Using a viscous or frozen solution, rotational correlation time (ϕ) increases and becomes much higher than the fluorescence lifetime of Trp. Under these conditions in the absence of segmental motion, anisotropy should approach the fundamental anisotropy of the Trp (Valeur and Weber 1977). But, if depolarization is detected, it reflects the existence of segmental motion. Indeed, the results revealed only intermediate emission anisotropy (Fig. 6) of the Trp emission in UeP dissolved in 80% glycerol at 0°C, where (ϕ) of 66 kDa (dimer of two 33 kDa) protein falls into microsecond range. Therefore, such depolarization reflects the presence of segmental motion or some rotational freedom of Trp located in the quasi- α -helices. The limiting anisotropy extrapolated from the Perrin plots obtained by varying temperature between 0 and 30°C was

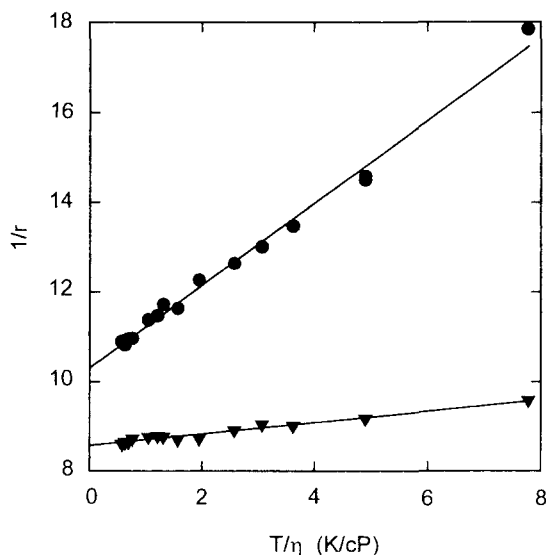


Figure 6. Perrin plots of emission anisotropies of the uncoupling protein tryptophans (●) Trp excited at 295 nm (▽) Trp excited at 300 nm. Reciprocal anisotropy $1/r$ of Trp emission (measured at 342 nm slit 8 nm) excited at 295 or 300 nm (slits 2 nm) in the isolated UCP dissolved in 80% glycerol and 20% of the isolation buffer was plotted against T/η ratio of absolute temperature T (which was varied) and viscosity η . Linear regressions were extrapolated to 0 at x axis and thereby yielded the limiting anisotropies r_0 of 0.097 or 0.117 for UCP tryptophans at 295 or 300 nm excitation respectively.

0.097 and 0.117 at excitation 295 (Fig. 6) and 300 nm (Fig. 6) (slit 1 nm) respectively. Note that the fundamental anisotropy of free tryptophan never reaches the theoretical limit of 0.4 but only 0.232 at excitation 295 and 0.307 at 300 nm (Valeur and Weber 1977). This is explained by the existence of torsional vibrations. On this basis, the axial depolarization factors $\langle d_D' \rangle$ calculated according to Dale et al. (1979) and Fanclough and Cantor (1978) reached values of 0.65 and 0.62 at 295 and 300 nm, respectively.

Discussion

This paper reports on a pilot photophysical study of a model integral membrane protein, the uncoupling protein. It has been shown that tryptophans located in the *transmembrane* segments might have properties rather similar to free tryptophan in water at pH 7 including two rotamers of zwitterionic form and the anionic form.

A common structural feature of integral membrane proteins consists in having

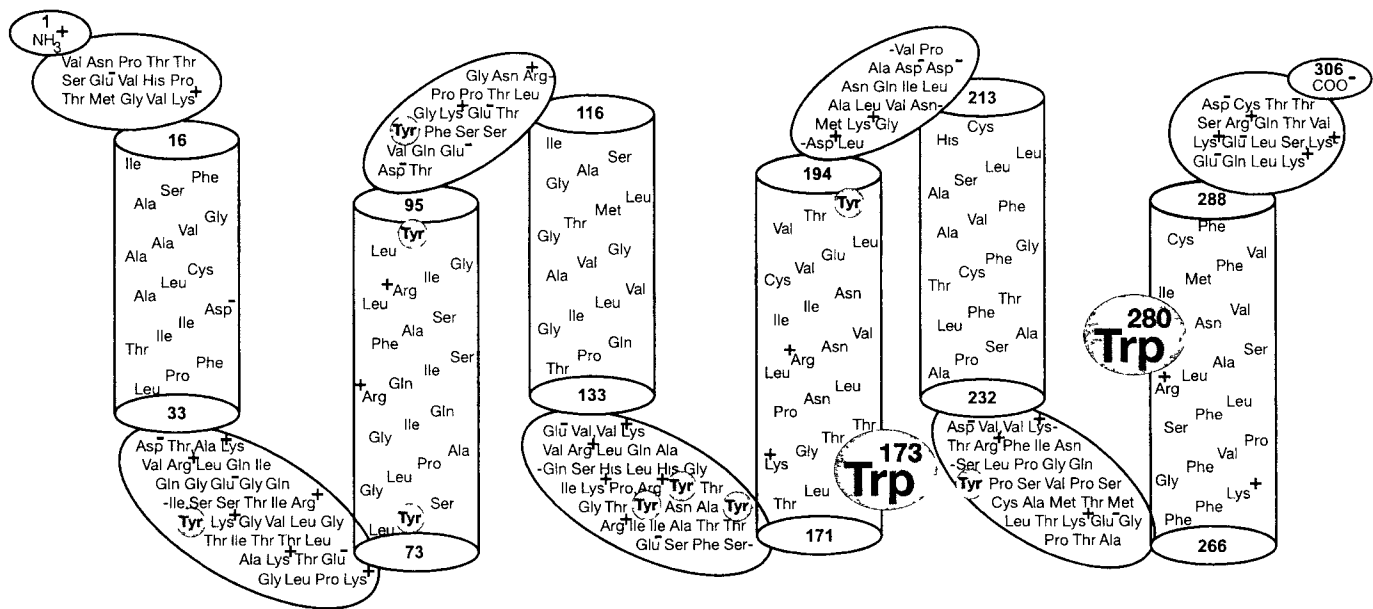


Figure 7. Photophysical map of the uncoupling protein. The model of transmembrane spanning was adopted from Klingenberg (1990) and Miroux et al (1992). Upper side represents the cytosolic side of the membrane; the bottom is the matrix side. The numbers indicate N-end and C-end position, and the residues that terminate the quasi α -helices, thereby being located at the water/lipid interface. Ionizable groups are marked by + or - signs. Notice that according to this model, the second, fourth, and sixth transmembrane α -helix contain two positive charges each. Both tryptophans, Trp-173 and Trp-280, and nine tyrosine residues are emphasized. At least four of the tyrosines are in the close neighborhood of Trp-173. A putative water-filled cavity forming the binding site for purine nucleotides (Mavinger and Klingenberg 1992; Modriansky et al 1997) should be located between all transmembrane segments, namely between the fifth and sixth α -helix and the third matrix sector protruding toward the central hydrocarbon region of the membrane. For the purpose of simplicity, Trp-280 is shown from the front view.

a certain number of membrane spanning segments, closely α -helical, intercepted by outer and inner hydrophilic segments. Most likely, the *trans*membrane helices are in contact with each other and this determines the basic structure. The existence of 50% α -helices in UCP is also supported by the interpretation of its Fourier-transform infrared spectra (Rial et al 1990), which also indicated 30% β -structure, 7% β -turns and 7% unordered. For UCP, a model of six-membrane-spanning α -helices (Klingenberg 1990, Fig. 7) has been partially verified experimentally by side-specific antibodies (Miroux et al 1992). Photophysically, tryptophan may have four different locations in an integral membrane protein: in hydrophilic segments, either exposed or unexposed to water environment, and in the transmembrane α -helices, either deeply embedded, or located near the water/lipid interface. The UCP contains just the two latter examples (Fig. 7). Trp-173 at the water/lipid interface, i.e. at the matrix end of the fourth *trans*membrane α -helix, and Trp-280 located in the middle of the sixth transmembrane α -helix, close to a cavity of the nucleotide binding site, identified among the fifth and sixth transmembrane α -helix (Mayinger and Klingenberg 1992, Murdza-Inghis et al 1994) and probably formed by most of the transmembrane α -helices (Modriansky et al 1997). In the UCP structure, there are also numerous Tyr residues located mostly in the water-exposed segments, namely in the matrix side (Fig. 7). Their extramembranous location and prevailing exposure to water environment were confirmed by revealing a quite intensive, red-shifted tyrosine emission of UCP, and by the second derivative absorption of UCP yielding an **a/b** ratio higher than 2/3.

In particular, the observed fluorescence of UCP tryptophans was characterized i) by only a slight blue-shift when compared to free tryptophan, ii) by low quantum yield, and iii) by a quite high depolarization factor. The last two properties are expected for Trp located in the 'breathing' *trans*membrane loops. Their dynamics is enhancing nonradiative decay processes, and is reflected by the observed axial depolarization factor of 0.6. But, instead of a blue-shift expected for intramembranous tryptophans, the corrected maximum of isotropic emission was found at 343 nm. Hence, both Trp-173 and Trp-280 should have prevailing contacts with hydrophilic residues, and both should be located close to water accessible space. In the case of Trp-280, it reflects the existence of the above mentioned water-filled cavity. Moreover, the obtained low quantum yield of 0.04 and 0.03 in intact and NEM-modified UCP, respectively, contradicts to locations of Trp in the regular α -helices that usually exhibit much higher quantum yields (Beechem and Brand 1985, Chabbert et al 1991). Also, the low quantum yield could originate from the presence of various residues participating in the overall quenching. A low quantum yield was also reported by Kawata and Hamaguchi (1991) in the case of the constant fragment of immunoglobulin.

The previous report of Viguiera et al (1992) suggested a very different accessibility of the two UCP tryptophans. On the basis of fluorescence-quenching-

resolved spectroscopy they suggested the existence of an iodide-inaccessible and denaturation-resistant Trp residue and of a second Trp residue responsible for the remaining 60% of total fluorescence that was quenched by iodide and was sensitive to denaturation. Because of its location in the membrane center, Trp-280 has been assigned to the putative iodide-inaccessible residue while the putative iodide-accessible residue with a higher quantum yield has been ascribed to Trp-173. Contrary to this, our measurements (Jeřek and Urbanková, unpublished data) with the single-Trp-containing mutants of UCP (Trp-173 or Trp-280 exchanged for Ala) showed that both tryptophans are quenched by iodide and that Trp 280 is actually more accessible.

Also, time-resolved fluorescence of UCP yielded decays that could be fitted by the three exponential components, accidentally similar to those reported for free tryptophan in water at pH 7. In the latter case, the shortest 0.5 ns and the 3 ns component were ascribed to the two respective rotamers of zwitterionic Trp (0.5 ns with a maximum at 330 nm, and 3 ns with a maximum at 315 nm) and the 10 ns component was assigned to anionic Trp (Creed 1984a; Beechem and Brand 1985). It can be speculated that in a flexible protein, Trp residue connected by the two peptide bonds represents the two conformers, identical to rotamers existing in the zwitterionic form of free tryptophan. This could lead to the presence of similar components (0.3–0.5 ns and 2–3 ns) in the UCP Trp emission decay. Also, a state similar to the state of anionic free tryptophan might be present in UCP, due to the possible existence of charge-transfer complexes between Trp-173 and Lys-174 and Trp-280 and Arg-276. The electron of the indole ring in the excited state can be more easily attracted by the positive charge of Lys-174 (Arg-276) and consequently, the radiation decay from such a state is delayed. This might explain the existence of the longest component of the UCP Trp emission decay. Note that lifetimes longer than 7 ns have been reported rather rarely for protein tryptophans (Beechem and Brand 1985; Schaefer and Gafni 1989; Peng et al. 1990). The exceptionally long (16 ns) lifetime of phosphoglycerate mutase Trp has been interpreted on the basis of static interactions between Trp and a second residue like His, Arg or Lys that perturbs both ground and excited states of the chromophore (Schaefer and Gafni 1989). The longest component in UCP Trp emission decay was delayed even more upon chemical modification with NEM. This modification, known to create conformational changes in UCP, caused further decrease in the quantum yield and led to an increase in the average lifetime without any change in emission spectrum. Therefore, this conformation change should be considered as quite weak, contrary to the proposal that it is a drastic change (Winkler and Klingenberg 1992). This is further confirmed by the only slightly altered exposure of Trp residues to water derived from the second derivative absorption (Fig. 2).

In general, the preferred interpretation of tryptophan emission decays in proteins includes rather an *a priori* existing ever-changing pattern of multimodal en-

energy transfer of all kinds, proceeding during the lifetime of the excited Trp state (Kim et al 1993). It is not necessary to consider the continuous distribution of lifetimes as in the case of the ground state microheterogeneity, when the inter-conversion rate between conformations is of the same order of magnitude as the excited-state decay rate (Alcala et al 1987; Szmajdzinski et al 1988). With our model example of an integral membrane protein it could be demonstrated that tryptophan residues, in spite of being located in the presumed α -helices, might exhibit properties of the two zwitterionic rotamers and the anionic form of free tryptophan. The most likely reason for the latter is the presence of charge-transfer complexes. Therefore we described another example supporting the point of view of Kim et al (1993).

Acknowledgements. This work was made possible by fellowships awarded by Spanish Academy of Sciences (C S I C) to Dr Petr Jezek to support his stage and measurements at Instituto de Química Física Rocasolano, C S I C, Madrid, Spain. The opportunity to use instruments at this institute and the advice and the stimulating discussions with Dr Ulises Acuña are gratefully acknowledged, as well as the possibility to prepare samples at the laboratory of Dr Eduardo Rial, Centro de Investigaciones Biológicas, C S I C, Madrid, Spain. Independent measurements in Prague were supported by grants from the Academy of Sciences of the Czech Republic, Grant No. A1011601, and by the Grant Agency of the Czech Republic, Grant No. 301/95/0620.

References

- Alcala J R, Gratton E, Prendergast F G (1987) Interpretations of fluorescence decays in proteins using continuous lifetime distributions. *Biophys J* **51**, 925–936.
- Azumi T, McGlynn S P J (1962) Polarization of the luminescence of phenanthrene. *J Chem Phys* **37**, 2413–2420.
- Beechem J M, Brand L (1985) Time-resolved fluorescence of proteins. *Annu Rev Biochem* **54**, 43–71.
- Bigelow D J, Inesi G (1991) Frequency-domain fluorescence spectroscopy resolves the location of maleimide-directed spectroscopic probes within the tertiary structure of the Ca-ATPase of sarcoplasmic reticulum. *Biochemistry USA* **30**, 2113–2125.
- Bishai F, Kuntz E, Augenstein L (1967) Intra- and intermolecular factors affecting the excited states of aromatic amino acids. *Biochim Biophys Acta* **140**, 381–394.
- Chabbert M, Lukas T J, Watterson D M, Axelsen P H, Prendergast F G (1991) Fluorescence analysis of calmodulin mutants containing tryptophan. Conformational changes induced by calmodulin binding peptides from myosin light chain kinase and protein kinase II. *Biochemistry USA* **30**, 7615–7630.
- Creed D (1984a) The photophysics and photochemistry of the near-UV absorbing amino acids. I. Tryptophan and its simple derivatives. *Photochem Photobiol* **39**, 537–562.
- Creed D (1984b) The photophysics and photochemistry of the near UV absorbing amino acids. II. Tyrosine and its simple derivatives. *Photochem Photobiol* **39**, 563–575.
- Dale R, Eisenger J, Blumberg W E (1979) The orientational freedom of molecular probes. The orientation factor in intramolecular energy transfer. *Biophys J* **26**, 161–194.

- Efting M R, Wasylewski Z, Ghiron C A (1987) Phase-resolved spectral measurements with several tryptophan containing proteins. *Biochemistry USA* **26**, 8338-8346
- Fanclough R H, Cantor C R (1978) The use of singlet-singlet energy transfer to study macromolecular assemblies. *Meth. Enzymol.* XLVIII, Part F: Enzyme Structure (Eds C H W Hiss, S N Timasheff) pp 347-379, Academic Press, New York
- Ferreira S T, Verjovsky-Almeida S (1989) Fluorescence decay of sarcoplasmic reticulum ATPase. Ligand binding and hydration effects. *J Biol Chem* **264**, 15392-15397
- Garlid K D, Orosz D E, Modriansky M, Vassanelli M, Jeřek P (1996) On the mechanism of fatty acid-induced proton transport by mitochondrial uncoupling protein. *J Biol Chem* **271**, 2615-2620
- Gonzalez-Manas J M, Lakey J H, Pattus F (1993) Interaction of the colicin-A pore-forming domain with negatively charged phospholipids. *Eur J Biochem* **211**, 625-633
- Hasselbacher C A, Rusmova E, Waxman E, Rusmova R, Kohanski R A, Lam W, Guha A, Du J, Lin T C, Polikarpov I, Boys C W G, Nemerson Y, Konigsberg W H, Ross J B A (1995) Environments of the four tryptophans in the extracellular domain of human tissue factor. Comparison of results from absorption and fluorescence difference spectra of tryptophan replacement mutants with the crystal structure of the wild type protein. *Biophys J* **69**, 20-29
- Jeřek P, Freisleben H-J (1994) Fatty acid binding site of the mitochondrial uncoupling protein. Demonstration of its existence by EPR spectroscopy. *FEBS Lett* **343**, 22-26
- Jeřek P, Garlid K D (1990) New substrates and competitive inhibitors of the Cl⁻-translocating pathway of the uncoupling protein of brown adipose tissue mitochondria. *J Biol Chem* **265**, 19303-19311
- Jeřek P, Modriansky M, Garlid K D (1997a) Inactive fatty acids are unable to flip-flop across the lipid bilayer. *FEBS Lett* **408**, 161-165
- Jeřek P, Modriansky M, Garlid K D (1997b) A structure-activity study of fatty acid interaction with mitochondrial uncoupling protein. *FEBS Lett* **408**, 166-170
- Jeřek P, Engstova H, Žáčkova M, Vercesi A E, Costa A D T, Arruda P, Garlid K D (1998) Fatty acid cycling mechanism and mitochondrial uncoupling proteins. *Biochim Biophys Acta* (in press)
- Kawata Y, Hamaguchi K (1991) Use of fluorescence energy transfer to characterize the compactness of the constant fragment of an immunoglobulin light chain in the early stage of folding. *Biochemistry USA* **30**, 4367-4373
- Kim S-J, Chowdhury F N, Stryjewski W, Younathan E S, Russo P S, Barkley M D (1993) Time-resolved fluorescence of the single tryptophan of *Bacillus stearothermophilus* phosphofructokinase. *Biophys J* **65**, 215-226
- Klemfeld A (1989) Tertiary structure of membrane proteins determined by fluorescence resonance energy transfer. In: *Spectroscopic Membrane Probes Vol I* (Ed L M Loew) pp 63-92, CRC Press Inc, Boca-Raton, Florida, USA
- Klingenberg M (1990) Mechanism and evolution of the uncoupling protein of brown adipose tissue. *Trends Biochem Sci* **15**, 108-112
- Ladokhin A S, Holloway P W (1995) Fluorescence of membrane-bound tryptophan octyl ester. A model for studying intrinsic fluorescence of protein-membrane interactions. *Biophys J* **69**, 506-517
- Ladokhin A S, Wang L, Stegles A W, Holloway P W (1991) Fluorescence study of a

- mutant cytochrome b₅ with a single tryptophan in the membrane binding domain *Biochemistry USA* **30**, 10200–10206
- Lakey J H, Baty D, Pattus F (1991) Fluorescence energy transfer distance measurements using site-directed single cysteine mutants. The membrane insertion of colicin A *J Mol Biol* **218**, 639–653
- Lakowicz J R (1984) *Principles of Fluorescence Spectroscopy* Chapter **11**, pp 341–379 Plenum Press, New York
- Lakowicz J R, Gryczynski I (1992) Tryptophan fluorescence intensity and anisotropy decays of human serum albumin resulting from one photon and two photon excitation *Biophys Chem* **45**, 1–6
- Lin C S, Klingenberg M (1982) Characteristics of the isolated purine nucleotide binding protein from brown fat mitochondria *Biochemistry USA* **21**, 2950–2956
- Mavinger P, Klingenberg M (1992) Labeling of two different regions of the nucleotide binding site of the uncoupling protein from brown adipose tissue mitochondria with two ATP analogs *Biochemistry USA* **31**, 10536–10543
- Miroux B, Casteilla L, Klaus S, Rambault S, Grandin S, Clement J-M, Ricquer D, Bouillaud F (1992) Antibodies selected from whole antiserum by fusion proteins as tools for the study of the topology of mitochondrial membrane proteins *J Biol Chem* **267**, 13603–13609
- Modriansky M, Murdza-Inghis D L, Patel H V, Freeman K B, Garlid K D (1997) Identification by site-directed mutagenesis of three arginines in uncoupling protein that are essential for nucleotide binding and inhibition *J Biol Chem* **272**, 24759–24762
- Murdza-Inghis D L, Modriansky M, Patel H V, Woldegiorgis G, Freeman K B, Garlid K D (1994) A single mutation in uncoupling protein of rat brown adipose tissue mitochondria abolishes GDP sensitivity of H⁺ transport *J Biol Chem* **269**, 7435–7438
- Nedergaard J, Cannon B (1992) The uncoupling protein thermogenin and mitochondrial thermogenesis. In *New Comprehensive Biochemistry: Molecular Mechanisms in Bioenergetics* (Ed L Ernster) Vol **23**, pp 385–420 Elsevier Science Publishers B V, Amsterdam
- Peng K, Visser A J W G, Van Hoek A, Wolfs C J A M, Hemminger M A (1990) Analysis of time-resolved fluorescence anisotropy in lipid-protein systems II. Application to tryptophan fluorescence of bacteriophage M13 coat protein incorporated in phospholipid bilayers *Eur Biophys J* **18**, 285–295
- Ragone R, Colonna G, Balestrieri C, Servillo L, Irace G (1984) Determination of tyrosine exposure in proteins by second-derivative spectroscopy *Biochemistry USA* **23**, 1871–1875
- Rial E, Muga A, Valpuesta J M, Arriondo J L, Goni F M (1990) Infrared spectroscopy studies of detergent-solubilized uncoupling protein from brown-adipose-tissue mitochondria *Eur J Biochem* **188**, 83–89
- Rodonova N A, Tatulian S A, Surrey T, Jahmig F, Tamm L K (1995) Characterization of two membrane-bound forms of OmpA *Biochemistry USA* **34**, 1921–1929
- Schanerle J A, Gafni A (1989) Long lived tryptophan fluorescence in phosphoglycerate mutase *Biochemistry USA* **28**, 3948–3954
- Shih T Y, Fasman G (1972) Circular dichroism studies of histone-deoxyribonucleic acid complexes. A comparison of complexes with histone I (f1), histone IV (f2a1) and their mixtures *Biochemistry USA* **11**, 398–404

- Szymanski H, Lakowicz J R, Johnson M L (1988) Time-resolved emission spectra of tryptophan and proteins from frequency-domain fluorescence spectroscopy. *SPIE* **909**, 293–298
- Valeur B, Weber G (1977) Resolution of the fluorescence excitation spectrum of indole into the 1L_1 and 1L_2 excitation bands. *Photochem Photobiol* **25**, 441–444
- Varley P G, Dryden D T F, Pam R H (1991) Resolution of the fluorescence of the buried tryptophan in yeast 3-phosphoglycerate kinase using succinimide. *Biochim Biophys Acta* **1077**, 19–24
- Viguera A R, Goni F M, Rial E (1992) The uncoupling protein from brown adipose tissue mitochondria. The environment of the tryptophan residues as revealed by quenching of the intrinsic fluorescence. *Eur J Biochem* **210**, 893–899
- Werner T C, Forster L T (1978) The fluorescence of tryptophyl peptides. *Photochem Photobiol* **29**, 905–914
- Winkler E, Klingenberg M (1992) Photoaffinity labeling of the nucleotide-binding site of the uncoupling protein from hamster brown adipose tissue. *Eur J Biochem* **203**, 295–304

Final version accepted May 12 1998